LOW-FREQUENCY INSTABILITY IN LIQUID-PROPELLANT ROCKET MOTORS

K. S. Kolesnikov

Zhurnal Prikladnoi Mekhaniki i Tekhnicheskoi Fiziki, No. 2, pp. 119-130, 1965

In the analysis of slow processes with characteristic time greatly exceeding the time of propagation of the pressure wave through the chamber, the working model used for liquid-propellant rocket motor (LRM) chambers is characterized by the fact that following injection all the fuel particles are converted into the end products of combustion in the time required for atomization, heating, vaporization, mixing, and chemical reaction. This time, which in a given model is the same for all fuel particles, is called the combustion time. For the simplest model the combustion time is independent of the chamber pressure.

Several mechanisms have been proposed for combustion instability in the chamber. One was first pointed out by Karman [1, 2]. It is based on the fact that the rate of propellant injection into the chamber has a delay relative to the pressure drop in the injectors of the order of the relaxation time of the feed line, while combustion follows the rate of injection with a lag equal to the combustion time. The half-period of the oscillations is approximately equal to the combustion time and the relaxation time of the system.

Another mechanism for the generation of low-frequency oscillations, which is independent of the process of propellant injection into the chamber and has therefore been called internal chamber instability, was proposed in [3]. It is based on the fact that the combustion time in the oscillating mode is also an oscillatory quantity. The combustion rate reaches a maximum when the rate of decrease of combustion time is greatest, and a minimum when the rate of increase of combustion time is greatest. If these oscillations coincide in phase with the pressure oscillations in the chamber, favorable conditions for self-excitation exist.

A detailed analysis of the simultaneous action of both excitation mechanisms was given in monograph [4].

Analysis of the stability of operation of a rocket motor, allowing for compressibility of the liquid in the feed line, for the simplest monopropellant system, shows that the critical delay time depends on the length of the line and decreases with the increase in the frequency of oscillation of the liquid in the line [5]. The best conditions for self-excitation occur when the frequency of oscillation in the feed line is close to one of the natural frequencies of the gases in the chamber. These oscillations are usually called high-frequency oscillations. The mechansim of high-frequency instability with constant rate of propellant injection into the chamber was examined in monograph [4] for purely longitudinal oscillations of the gases.

The stability of operation of LRM depends on the elastic properties of the vehicle in which the motor is mounted. There is severe additional feedback between the combustion chamber and the feed lines through the elastic vehicle structure. This question was examined in [6] with reference to a monopropellant system with an incompressible fuel.

The case may arise in practice when the natural frequencies of the wave processes in the feed lines are of the same order as or lower than the oscillation frequencies determined by the combustion time. This becomes especially important if the characteristic frequencies of the elastic oscillations of the vehicle structure, or of the test bed on which the chamber is mounted, are close to the frequencies of the wave processes in the feed lines. Such cases are examined below.

In this paper the concepts of low-frequency instability of LRM are further developed. A closed system may be unstable even if the combustion time is zero. The frequency of this type of instability is determined by the time of propagation of elastic waves in the feed lines and in the structure and may vary widely. The combustion time affects the phase relations and may be an additional cause of excitation of oscillations.

The dynamic system consists of separate elements joined on the basis of the boundary conditions. Determination of the parameters of these elements is, generally speaking, an independent and very complex problem. The closed system, represented by a block diagram, is of the multiloop type. The transfer functions of the feed lines are obtained in a form such that their coupling with the vehicle structure is complete. A solution is obtained in the linear formulation, and the properties of the transfer functions of the separate elements and of the system as a whole are analyzed using the special methods of automatic control theory.

1. We shall assume that for low-frequency oscillations: a) the gas pressure p_3 at each moment of time is practically the same throughout the chamber, b) the combustion time τ^0 is the same for all fuel particles, c) the gas flow through the nozzle is quasi-steady. The following linearized mass balance equation for the chamber gases was obtained in [3]:

$$\frac{d\beta}{dz} + (1-\nu)\beta + \nu\beta(z-\tau^*) = A[\mu_1(z-\tau^*-1) - \mu_2(z-\tau^*-1)] + \\ + (1/2 - H - 2A)\mu_1(z-\tau^*) + (1/2 + H + 2A)\mu_2(z-\tau^*), \tag{1.1}$$

where

$$\beta = \frac{p_3 - p_3^\circ}{p_3} \qquad \mu_1 = \frac{m_1 - m_1^\circ}{m_1^\circ}, \qquad \mu_2 = \frac{m_2 - m_2^\circ}{m_2^\circ}, \\ H = \frac{1}{2}\frac{r-}{r-} \qquad r = \frac{m_2^\circ}{m_1^\circ}, \qquad z = \frac{t}{\theta}, \qquad \tau^* = \frac{\tau^\circ}{\theta}, \tag{1.2}$$

m_2, m_1 are the mass injection rates of oxidizer and fuel; p_3°, m_2°, m_1° are the chamber pressure and the mass injection rates of oxidizer and fuel in the undisturbed regime; θ is the chamber relaxation time; ν is a factor representing the interaction between the combustion process and the oscillations in the combustion chamber.

The coefficient A allows for the effect of temperature oscillations. It characterizes the chosen propellants and depends on the ratio r of their mass flow rates in the undisturbed regime and on the chamber pressure. For ordinary bipropellant motors, A is a very small positive quantity.

In analyzing the low-frequency instability of a closed system it is of interest to examine in the first approximation the simple chamber model in which combustion time τ° is independent of pressure ($\nu = 0$), while the gas temperature in the chamber is constant irrespective of the pressure oscillations and the propellant ratio (A = 0),

$$\frac{d\beta}{dz} + \beta = (1/2 - H)\mu_1(z-\tau^*) + (1/2 + H)\mu_2(z-\tau^*). \tag{1.3}$$

This model is similar to that of a monopropellant system, but if the properties of the oxidizer and fuel lines are different, it may be expected that the bipropellant system will be considerably more complex.

The dimensionless variations μ_1, μ_2 must be determined from dynamics of the oxidizer and fuel lines.

We shall express the dynamic properties of the combustion chamber in terms of complex ratios. Since the variation of propellant injection into the chamber is assumed to be harmonic, taking into account the delay arguments $z - \tau^*$ and $z - \tau^* - 1$, we have [7]

$$\mu_1(z-\tau^*) = \mu_1(z)e^{-is\tau^*} = \mu_1 e^{is(z-\tau^*)} \qquad (sz = \Omega t,\ s = \Omega\theta), \\ \mu_1(z-\tau^*-1) = \mu_1 e^{is(z-\tau^*-1)}.$$

Here Ω is the oscillation frequency. We shall seek a solution of (1.1) in the form

$$\beta(z) = \beta e^{isz}, \qquad \beta(z-\tau^*) = \beta e^{is(z-\tau^*)}.$$

Then the complex ratios giving the relation between the output and the input coordinates are found from the expressions

$$\mathbf{K}[\beta, \mu_1] = \beta/\mu_1 = d_1/d, \qquad \mathbf{K}[\beta, \mu_2] = d_2/d, \\ d = \nu + (is + 1 - \nu)e^{is\tau^*}, \qquad d_1 = 1/2 - H - 2A + Ae^{-is}, \\ d_2 = 1/2 + H + 2A + Ae^{-is}. \tag{1.4}$$

Hodographs of the vectors $\mathbf{K}[\beta, \mu_1]$, $\mathbf{K}[\beta, \mu_2]$ in the complex plane $Z = U + iV$ in the interval $0 \leqslant s \leqslant \infty$ are spirals contracting toward the origin of coordinates. The smaller τ^*, the more the spiral is compressed, and the less the phase delay φ for given values of s. These are typical aperiodic elements of the first order with delay.

Graphs of the hodographs of the vectors $\mathbf{K}[\beta, \mu_2]$ for H = 0.214 are shown in Figs. 1 and 2. Curves 1 and 2 are plotted for A = ν = 0, curve 1 corresponding to τ^* = 0.5 and curve 2 to τ^* = 1.5. Figure 2 shows the effect of the coefficient A. In this case the graphs are plotted for τ^* = 0.5 and ν = 0, curve 3 being for A = 0, curve 4 for A = 0.05, and curve 5 for A = 0.1. If it is assumed, for example, that A = 0, ν = 0.2, the graph practically coincides with curve 3.

For small values of s, the coefficient ν has almost no effect either on the modulus or on the argument of the complex ratio, while increase of A leads to increase of the modulus, the argument remaining almost unchanged.

2. Variation of the pressure in the combustion chamber causes a variation in vehicle acceleration, or, if the LRM is mounted on a nonrigid test bed, a change in the strains in the bed, including the propellant lines. In both cases the motion of the structure and of the attached propellant lines leads to a change in pressure upstream from the combustion chamber injectors.

Let us examine the disturbed motion of the vehicle structure. The undisturbed (design) mode of the system corresponds to the condition when the supply of fuel to the combustion chamber and the motor thrust are constant with the vehicle in straight flight. Since over tens of cycles of the oscillations studied the mass of the vehicle hardly changes

from fuel expenditure, we shall "freeze" the coefficients of the equations of motion, i. e., the level in the propellant tanks, the mass of the vehicle, and the frequency and shape of the natural elastic oscillations of the structure over short intervals will be considered first.

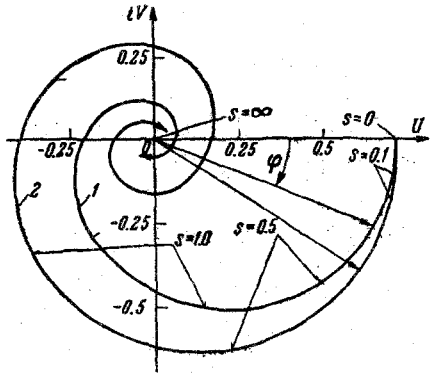

Fig. 1

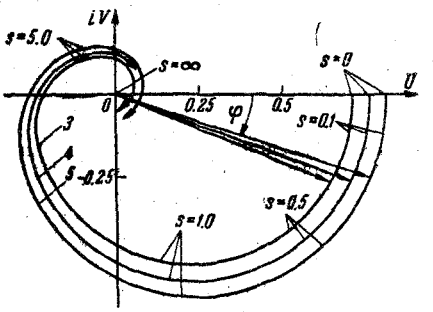

Fig. 2

The variation of the displacement of any cross section of the structure in the direction of its longitudinal axis may be represented in the form of the sum

$$q(x, t) = q_c(t) + \sum_{n=1}^{\infty} f_n(x)\, q_n(t). \qquad (2.1)$$

Here $q_c(t)$ is the variation of the displacement of the center of mass of the vehicle, $f_n(x)$ is the shape of the n-th normal harmonic of the longitudinal oscillations of the structure, $q_n(t)$ is the displacement of the relative center of mass for oscillations of the n-th harmonic of the section for which $f_n(x) = 1$.

Determination of the natural frequencies Ω_n and the characteristic functions $f_n(x)$ for an elastic structure is an independent complex problem and will not be discussed here. We shall consider these data to be known and choose the frame of reference so as to satisfy the relation

$$\int_0^l m(x)\, f_n(x)\, dx + \sum_{k=1}^{N} m_k f_{nk} = 0 \qquad (k = 1, 2, \ldots, N). \qquad (2.2)$$

in which l, $m(x)$ are the length and mass per unit length of the structure, and m_k are concentrated masses. In the first approximation, these masses may be taken to be those of the motor, the propellant pumps, the propellants in the tanks, etc., which, as a rule, are elastically connected with the walls.

Oscillations in the propellant lines cannot, in practice, cause longitudinal oscillations of the structure, and therefore the latter are due only to variation in thrust.

We denote by m the mass of the vehicle, by Ω the frequency of the natural elastic longitudinal oscillations of the structure, and by k° the proportionality factor between the variations of chamber pressure and thrust. We assume that the thrust vector coincides with the longitudinal axis of the structure. Then, from (2.1) and (2.2), the linearized equations of perturbed motion of the center of mass of the vehicle and elastic oscillation of the structure relative to the center of mass may be written in the form

$$\frac{d^2 q_c(t)}{dt^2} = \frac{k^\circ p_3^\circ}{m}\beta, \qquad \frac{d^2 q_n(t)}{dt^2} + \Omega_n^2 q_n(t) = \frac{k^\circ p_3^\circ f_{nv}}{m_n}\beta. \qquad (2.3)$$

Here m_n is the reduced mass of the structure, and f_{nv} is the value of the characteristic function at the section where the chamber pressure is converted into thrust. For the sake of definiteness, we shall identify this section with the injector head;

$$m_n = \int_0^l m(x)\, f_n^2(x)\, dx + \sum_{k=1}^{N} m_k f_{nk}^2.$$

We introduce the dimensionless displacements and times

$$\eta_c = \frac{q_c}{l}, \qquad \eta_n = \frac{q_n}{l}, \qquad \sigma = t\frac{a_0}{l},$$

where a_0 is the reduced speed of sound in the elastic structure.

Keeping in mind the fact that $\beta(z) = \beta \exp isz$, $sz = \Omega t = \omega\sigma$, we may write the solution of (2.3) in the form

$$\eta_c(\sigma) = \eta_c e^{i\omega\sigma}, \qquad \eta_n(\sigma) = \eta_n e^{i\omega\sigma}.$$

The relations between η_c, η_n and β are expressed by the ratios

$$\mathbf{K}[\eta_c, \beta] = -\frac{k^*}{\omega^2}, \qquad \mathbf{K}[\eta_n, \beta] = \frac{k_n}{\omega_n^2 - \omega^2}. \tag{2.4}$$

The dimensionless natural frequency ω_n and the amplification factors k^*, k_n are given by

$$\omega_n = \Omega \frac{l}{a_0}, \qquad k^* = \frac{k^\circ p_3^\circ l}{m a_0^2}, \qquad k_n = k^* \frac{m}{m_n} f_{nv}. \tag{2.5}$$

For frequency variation in the range $0 \leqslant \omega \leqslant +\infty$, the hodographs of vectors $\mathbf{K}[\eta_c, \beta]$ $\mathbf{K}[\eta_n, \beta]$ in the complex plane $Z = U + iV$ will be straight lines coincident with the real axis.

Due to energy dissipated in the material and joints of the structure, the natural oscillations of the latter are always damped, and so infinitely great values of the vector $\mathbf{K}[\eta_n, \beta]$ are not physically possible at $\omega = \omega_n$. When it is necessary to determine the oscillations at resonance, resistances proportional to the first power of velocity are introduced into the elastic oscillation equations.

In this case the ratio $\mathbf{K}[\eta_n, \beta]$ will be complex

$$\mathbf{K}[\eta_n, \beta] = k_n / D_n, \qquad D_n = \omega_n^2 - \omega^2 + 2\varepsilon_n i\omega, \tag{2.6}$$

where ε_n is the damping factor for the natural oscillations.

The stability analysis is simplified if the forced oscillations of the structure are not expanded as a series in the characteristic functions $f_n(x)$, but are represented in the form

$$q(x, t) = \beta(z)\, lf\left(\frac{x}{l}, \omega\right) = \beta l f(\xi, \omega)\, e^{i\omega\sigma}, \tag{2.7}$$

where $f(\xi, \omega)$ is the shape of the forced oscillations. For a nonuniform rod with a stepwise change in mass and stiffness along its length, even with elastically suspended concentrated masses, the functions $f(\xi, \omega)$ without allowance for energy dissipation, have real values and prove to be comparatively simple. There are no essential difficulties in determining these functions, and therefore the forced oscillations of the structure may be treated in the form (2.7) instead of (2.1). When energy dissipation is considered, the functions $f(\xi, \omega)$ are complex.

3. We shall assume for purposes of analysis that the propellant system is one in which the propellants are delivered from the tanks to the combustion chamber by pumps. This system is common in high-thrust motors and includes as a special case systems in which the driving force is compressed gas. The liquid propellants and the supply lines are not absolutely rigid, but have a certain elasticity which may be shown to have a considerable influence on the oscillatory processes in the lines.

The oxidizer and fuel lines are identical in structure. Each consists of three elements connected in series; pipes leading from the tank to the pump, the pump, and pipes leading from the pump to the injectors [8]. The first pipe is in many instances straight and uniform, while the second is usually more complex in shape. It includes a valve, the motor head space, and, for the coolant, an additional system of branched pipes and a narrow passage. The situation is not one characterized by a regular geometry, which would allow an exact solution of the problem of combined oscillation of the elastic volume and the liquid. Because of the elasticity of the propellant lines, however, their volume varies with variation of pressure, so that a variation of propellant injection into the combustion chamber does not coincide with a variation in flow through the pump. The quantitative differences depend on propellant line volume and the ratio of oscillation frequencies.

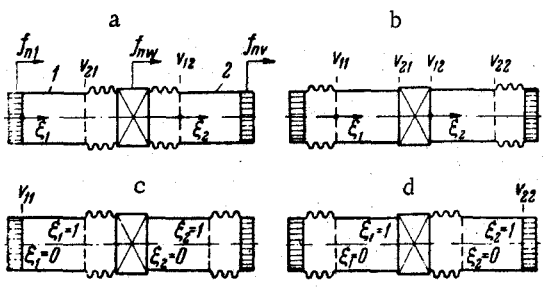

Fig. 3

To solve the hydrodynamic problem, we replace the line joining the pump to the chamber with a model in the form of a straight tube of constant cross section. We assume, in the first approximation, that the injector head and the inner walls of the chamber are rigid. Then pressure variation in the chamber will not cause a change in volume of the propellant lines, which will vary only due to the elasticity of the outer walls. In actuality, the inner walls of the chamber and the injector head have some compliance, and if this is commensurate with that of the outer walls or of the liquid, it must be taken into account.

The model for the oxidizer and fuel lines thus consists of two straight uniform tubes between which the pump is mounted. There may be compensating bellows at the ends of the tubes, with negligible rigidity in the axial direction (Fig. 3). In our model we shall consider the bellows as a volume, at any point of which the pressure variation is the same, while the volume variation is proportional to the pressure variation and the change in distance between end sections.

The propellant lines are connected to the structure: the near end of the first tube is joined to the bottom of the tank the far end of the second tube is joined to the injector head of the combustion chamber, while the pump is suspended from the structure on a frame or attached to the combustion chamber [8]. The propellant lines undergo forced oscillations, whose nature is determined by motion of the corresponding sections of the structure. The presence of the bellows allows the tubes and the pump to oscillate at different amplitudes.

We denote the characteristic functions as follows: f_{n1} for the flange at the bottom of the tank, f_{nw} for the pump, and f_{nv} for the injector head. Since the bottom of the tank and the thrust frame have some elasticity, the values of functions f_{n1}, f_{nw}, f_{nv} are not the same as the values of the functions for the corresponding frames of the structure. The difference is the greater, the closer the natural oscillation frequency of the structure and the partial oscillation frequencies of the bottom of the tank with the propellant, the motor, and the pump. The values of functions f_{n1}, f_{nw}, f_{nv} may be modified to some extent by design measures and may therefore be related to a number of variable parameters of the system.

The hydrodynamic problem for the propellant lines is to determine the variation of propellant injection into the chamber as a function of the small longitudinal oscillations of the structure and the variation of chamber pressure.

We assume that the propellants are perfect liquids, and that the undisturbed flow in the tubes is uniform – velocity v_0, pressure p_0 and density ρ_0 constant; we allow for the elasticity of the tubes via the reduced speed of sound.

Since the equivalent tubes are assumed to be rigid, and friction between the liquid and their walls is not allowed for in the calculation, small movements of the tubes in the axial direction do not affect the flow velocity.

The effect on liquid flow of the motions of injector head, pump, and tank bottom, and also changes in the volumes of the bellows are treated as perturbations of the boundary conditions. In view of our assumption that the undisturbed motion is quasi-steady, the hydrodynamic problem may be solved as if the tubes were motionless.

We shall employ the method of solution proposed in [13], introducing analogous notation. We denote the dimensional variations of pressure and velocity in the j-th tube by p_{xj}, v_{xj}, the coordinate of the flow cross section in the j-th tube by x_j, and the time by t, with the following relations between the dimensional and the dimensionless quantities:

$$v_j = \frac{v_{xj}}{a_{0j}}, \quad p_j = \frac{p_{xj}}{\rho_{0j} a_{0j}^2}, \quad s_j = \Omega \frac{l_j}{a_{0j}}, \quad \tau_j = t \frac{a_{0j}}{l_j}, \quad \xi_j = \frac{x_j}{l_j},$$

where a_{0j} is the speed of sound in the undisturbed flow, and l_j is the length of the j-th tube. For the tube leading to the pump, j = 1, and beyond the pump j = 2.

Let us examine the boundary conditions. If the pressure of the gases above the surface of the liquid in the tank remains unchanged in the presence of oscillations of the structure, pressure perturbations at the outlet from the tank to the tube will be caused only by oscillations of the tank bottom. Neglecting wave formation at the free surface in the tank, we may write

$$p_x = \rho_{01} h_1 \frac{d^2}{dt^2} \left[q_c(t) + \sum_{n=1}^{\infty} \varkappa_n f_{n1} q_n(t) \right].$$

Here ρ_{01}, h_1 are the density and the height of the column of liquid in the tank; $\varkappa_n$ is some coefficient depending on the ratio of the diameters of tank and tube, the shape of the bottom, and the conditions of liquid flow from tank to tube. We divide this variation by $\rho_{01} a_0^2$ – the parameters of the undisturbed flow in the tube ahead of the pump. We obtain

$$p^* = -\omega^2 (N_c \eta_c + \sum_{n=1}^{\infty} N_n \eta_n), \quad p^* = \frac{p_x}{\rho_{01} a_{01}^2}, \quad N_c = \frac{h_1 a_0^2}{l a_{01}^2}, \quad N_n = N_c \varkappa_n f_{n1}. \qquad (3.1)$$

The velocity variations at the ends of the tubes are determined from the conditions of flow continuity in the propellant lines. They depend on the properties and locations of the bellows.

We express the properties of the bellows by means of two independent dimensionless parameters. The geometry parameter λ_j takes account of the variation in the geometry of the corrugations and in the cross-sectional area of the bellows.

$$\lambda_j = \frac{1}{F_{0j}} \left(\frac{\partial V_{xj}}{\partial x} \right)_{x = x_{0j}} - 1.$$

Here F_{0j} is the flow-passage cross-sectional area of the j-th tube, V_{xj} is the volume of the bellows, x_{0j} is the distance between the ends of the bellows under undisturbed flow conditions.

The elastic parameter r_j takes account of variation of the compensator volume due to pressure variation

$$r_j = r_{xj}\frac{a_{0j}^2\rho_{0j}}{F_{0j}l_j} \qquad \left(r_{xj} = \left[\frac{\partial V_{xj}}{\partial p_x}\right]_{p_x=p_{0j}}\right).$$

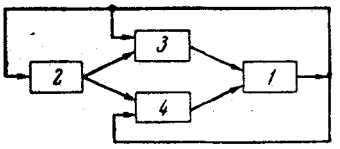

Fig. 4

The geometry of the corrugations of the bellows varies in proportion to the difference of the values $f_{nw} - f_{n1}$ and $f_{nv} - f_{nw}$. We introduce additional subscripts for the bellows parameters, pressures, and velocities at the ends of the tubes: 1 – for the tube inlet, 2 – for the tube outlet.

We take a_{02} as the scale of the dimensionless variation w of the flow velocity through the pump and write the dimensionless variations of generalized velocities of the structure as

$$u_c = -\frac{1}{a_{02}}\frac{dq_c(t)}{dt} = -i\omega\frac{a_0}{a_{02}}\eta_c, \qquad u_n = -\frac{1}{a_{02}}\frac{dq_n(t)}{dt} = -i\omega\frac{a_0}{a_{02}}\eta_n. \tag{3.2}$$

Since a positive displacement of the structure q(x, t) has been assumed to correspond to displacement in a direction opposite to the positive direction of the velocity v_j of liquid flow in the tubes, "minus" signs have been introduced in (3.2).

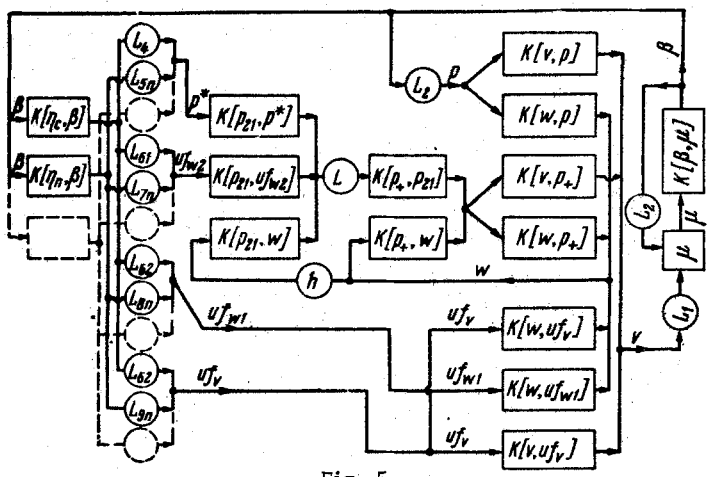

Fig. 5

Taking $p_j(\xi_j, \tau_j) = p_j(\xi_j)\exp is_j\tau_j$ and denoting by $v\exp is_2\tau_2$ the variation, divided by a_{02}, of the rate of injection of liquid into the chamber $h = a_{02}/a_{01}$, we form the equations of continuity. In order to make fuller use of the results of the solution [9], we write them in the form

$$\begin{aligned} v_{21} &= wh + huf_{w2} + is_1r_{21}p_{21}, \\ v_{21} &= w + uf_{w1} - is_2r_{12}p_{12}, \\ v_{22} &= v + uf_v + is_2r_{22}p_{22}, \end{aligned} \tag{3.3}$$

where uf_{w2}, uf_{w1}, uf_v are the velocities described by the motion of the characteristic sections of the propellant lines together with the structure.

There may be some gas volumes on the suction side of the pump due to cavitation effects [10]. Assuming that the variation of these volumes is inversely proportional to the pressure variation upstream from the pump, the equations of continuity of flow in the propellant lines will have the same form, if we understand r_{21} to denote the generalized elastic characteristic of the bellows combined with the gas volumes.

Possible arrangements of the bellows in the propellant lines are illustrated in Fig. 3. For Fig. 3a

$$\begin{aligned} uf_{w2} &= u_c + \sum_{n=1}^{\infty}\left[f_{nw}(1+\lambda_{21}) - \lambda_{21}f_{n1}\right]u_n, \\ uf_{w1} &= u_c + \sum_{n=1}^{\infty}\left[f_{nw}(1+\lambda_{12}) - \lambda_{12}f_{nv}\right]u_n, \end{aligned} \tag{3.4}$$

For Figs. 3b and 3c

$$uf_v = u_c + \sum_{n=1}^{\infty} [f_{nv}(1 + \lambda_{22}) - \lambda_{22} f_{nw}]\, u_n . \tag{3.5}$$

The expressions uf_{W2} for Figs. 3b, d, uf_{W1} for Figs. 3b, c, and uf_V for Figs. 3a, d may be obtained from (3.4) and (3.5), by putting the coefficients λ_{21}, λ_{12}, λ_{22}, respectively, equal to zero. In this case we must put the coefficients r_{21}, r_{12}, r_{22} equal to zero in (3.3).

When the bellows are located between the tube and the tank (Fig. 3b, d), the variation of flow velocity at the outlet from the tank will differ from the variation v_{11} of velocity at the inlet to the tube, and therefore the variation of the pressure drop $p^* - p_{11}$ will be expressed by the relation

$$p^* - p_{11} = \psi_1 M_1 \left\{ v_{11} - \sum_{n=1}^{\infty} [f_{n1}(1 + \lambda_{11}) - f_{nw}\lambda_{11}] + is_1 r_{11} p_{11} \right\}, \tag{3.6}$$

where ψ_1 is the resistance coefficient, referred to the velocity, at the outlet from the tank.

For Figs. 3a and 3c

$$p^* - p_{11} = \psi_1 M_1 v_{11} \quad \left(M_1 = \frac{v_{01}}{a_{01}} \right).$$

We may also use (3.4) and (3.5) in the case when the motion of the structure is represented in the form (2.7). In this case we must put $u_c = 0$ and instead of infinite sums of the characteristic functions simply take the differences of the shapes of the forced oscillations

$$\begin{aligned} uf_{w2} &= -i\omega \frac{a_0}{a_{01}} \beta [f(\xi_w, \omega)(1 + \lambda_{21}) - f(\xi_1, \omega)\lambda_{21}], \\ uf_{w1} &= -i\omega \frac{a_0}{a_{02}} \beta [f(\xi_w, \omega)(1 + \lambda_{12}) - f(\xi_v, \omega)\lambda_{12}], \\ uf_v &= -i\omega \frac{a_0}{a_{02}} \beta [f(\xi_v, \omega)(1 + \lambda_{22}) - f(\xi_w, \omega)\lambda_{22}], \end{aligned} \tag{3.7}$$

where $f(\xi_1, \omega)$, $f(\xi_w, \omega)$, $f(\xi_v, \omega)$ are the shapes of the forced oscillations of the flange at the bottom of the tank, the pump, and the injector head.

By introducing the summing factors uf_{w2}, uf_{w1}, uf_v, we have reduced the propellant supply scheme and the boundary conditions of the problem to the structure investigated in detail in [9]. The results of that paper are used here without being set out. The formulas for the complex ratios $\mathbf{K}[p_{21}, p^*]$, $\mathbf{K}[p_{21}, w]$, $\mathbf{K}[v, p_{12}]$, $\mathbf{K}[v, p]$, $\mathbf{K}[w, p]$, $\mathbf{K}[w, p_{12}]$ retain their previous form, and the formulas for $\mathbf{K}[p_{21}, uf_{w2}]$, $\mathbf{K}[v, uf_v]$, $\mathbf{K}[w, uf_{w1}]$, $\mathbf{K}[w, uf_v]$ may be obtained from the expressions $\mathbf{K}[p_{21}, u]$, $\mathbf{K}[v, u]$, $\mathbf{K}[w, u]$, given in [9] by putting $f_{w1} = f_{w2} = f_v = 1$. Instead of one block $\mathbf{K}[w, u]$ there will be two parallel blocks with ratios $\mathbf{K}[w, uf_v]$ and $\mathbf{K}[w, uf_{w1}] = -1$. This difference arises from the fact that, in general, variation of the geometry of the bellows of the second tube is the result of two simultaneous displacements – of the pump and of the injector head.

The ratios for the first tube will be expressed by other formulas, if the bellows are located between the tube and the tank (Figs. 3b, d). They may be obtained from (3.6) by the method described in [9]. The influence of the location of the bellows on the dynamic properties of the propellant line becomes noticeable if the compliances r_{11} and r_{21} of the bellows are considerable, or if the geometric characteristics $|\lambda_{11}| \gg 0$, $|\lambda_{21}| \gg 0$.

4. A block diagram of the physical elements is shown in Fig. 4. Here 1) is the chamber, 2) the vehicle structure (or test bed), 3) the fuel line, 4) the oxidizer line. Perturbation of the motion of the structure causes a variation of pressure in the propellant lines and hence a variation of propellant injection into the chamber. A pressure variation develops in the combustion chamber, affecting the propellant lines and the motion of the structure. The system is thus a closed one and, moreover, has positive feedback.

Figure 5 shows an expanded block diagram which includes only one propellant line. A second propellant line should be connected in accordance with Fig. 4. The motion of the structure is assumed to take the form (2.1). Here only one element is shown for the n-th harmonic of the oscillations of the structure. In fact n = 1, 2, 3..., the elements being located in parallel, as shown by the broken lines.

The system has three internal feedbacks: between the chamber and the second tube – pressure $p = L_2\beta$, between the second and the first tube – velocity w; the third feedback involves the chamber, and results from the fact that the chamber transfer function depends on mass propellant injection rate, while the propellant injection rate serves as an output coordinate for the tube.

Since the dimensionless parameters of the physical elements are different, while the variation of the boundary conditions at the ends of each tube is determined by the displacements of two sections of the structure, scale factors and summing factors have been introduced to connect the elements into the over-all scheme. The composition of the summing factors uf_{w2}, uf_{w1} and uf_v for Fig. 5 is determined by (3.4) and (3.5).

The variation of the mass injection rate of propellant into the chamber depends on the variation of velocity v and the variation of density ρ_{22} at the right-hand end of the second tube. Thus, for the oxidizer, for example, we have

$$m_2 = (v_0 + a_{02}v)(1 + p_{22})\rho_{02}F_{02}, \qquad m_2^\circ = v_{02}\rho_{02}F_{02}.$$

Retaining only small quantities of the first order and noting that $p_{22} = \rho_{22}$, on the basis of (1.2) we obtain

$$\mu_2 = p_{22} + \frac{v}{M_2}.$$

It is convenient to express pressure p_{22} with the help of formula (2.12) from [9] for j = 2. Noting that $p\rho_{02}a_{02}^2 = \beta p_3^\circ$, we have

$$\mu_2 = L_1 v + L_2\beta, \qquad L_1 = (M_2^{-1} + \psi_2 M_2), \qquad L_2 = p_3^\circ / \rho_{02}a_{02}^2. \tag{4.1}$$

On the basis of (3.1) we conclude that

$$L_4 = -\omega^2 N_c, \qquad L_{5n} = -\omega^2 N_n. \tag{4.2}$$

We find expressions for the coefficients L_{61}, L_{62}, L_{7n}, L_{8n}, L_{9n} from a comparison of (3.2) with (3.4) and (3.5)

$$\begin{aligned} L_{61} &= -i\omega a_0 / a_{01}, \qquad L_{62} = -i\omega a_0 / a_{02}, \\ L_{7n} &= L_{61}[f_{nw}(1 + \lambda_{21}) - \lambda_{21}f_{n1}], \\ L_{8n} &= L_{62}[f_{nw}(1 + \lambda_{12}) - \lambda_{12}f_{nv}], \\ L_{9n} &= L_{62}[f_{nv}(1 + \lambda_{22}) - \lambda_{22}f_{nw}], \end{aligned} \tag{4.3}$$

The part of the block diagram, corresponding to the representation of the displacements of the structure in the form (2.7), is shown in Fig. 6. Instead of an infinite number of blocks expressing the dynamic properties of the structure, there are only three, which is an advantage in analyzing the system. The expressions uf_{w2}, uf_{w1}, uf_v are determined from (3.7) while the variation of pressure p* is calculated from

$$p^* = L_3 f(\xi_1, \omega)\beta, \quad L_3 = -\omega^2\frac{h_1 a_0^2 \varkappa(\omega)}{a_{01}^2 l}. \tag{4.4}$$

where the coefficient $\varkappa(\omega)$ depends on the oscillation frequency and is referred to the total variation of the displacement of the flange at the bottom of the tank. The remainder of the block diagram is the same as in Fig. 5.

If the geometry of the bellows is such that we may assume $\lambda_{12} = \lambda_{21} = \lambda_{22} = 0$, the velocities uf_{w2}, uf_{w1}, uf_v are determined on the basis of (3.7) without summation and the block diagram is simplified. The variant of the modified part of the block diagram corresponding to this case is shown in Fig. 7.

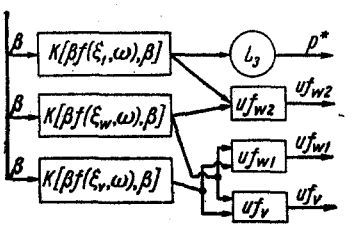

Fig. 6

Here the oscillations $\beta f(\xi_1, \omega)$ of the tank bottom cause only a variation of the pressure p* at the inlet to the first tube, the oscillations $\beta f(\xi_w, \omega)$ of the pump affect the velocity of the liquid at the outlet from the first tube and at the inlet to the second, and the oscillations $\beta f(\xi_v, \omega)$ of the injector head affect the velocity of the liquid at the outlet from the second tube.

The relations between the dimensionless oscillation frequencies for the various elements are established from the equalities

$$\Omega = \frac{s}{\theta} = \omega\frac{a_0}{l} = s_1\frac{a_{01}}{l_1} = s_2\frac{a_{02}}{l_2}.$$

Hence

$$\begin{aligned} s &= s_1 q, \qquad s_2 = s_1 q_2, \qquad \omega = s_1 q_1 \\ q &= \theta\frac{a_{01}}{l_1}, \qquad q_1 = \frac{l}{l_1}\frac{a_{01}}{a_0}, \qquad q_2 = \frac{l_2}{l_1}\frac{a_{01}}{a_{02}}. \end{aligned} \tag{4.5}$$

The multiloop system shown in Fig. 5 may be simplified by replacing the elements with feedback circuits by their equivalents without feedback. An example of this substitution is shown in Fig. 8. The equivalent element with complex ratio $\mathbf{K}^*[\beta, v]$ expresses the relation between the variation of chamber pressure and the variation of propellant injection rate:

$$\mathbf{K}^*[\beta, v] = \frac{\mathbf{K}[\beta, \mu] L_1}{1 - \mathbf{K}[\beta, \mu] L_2}. \qquad (4.6)$$

The hodograph of vector $\mathbf{K}^*[\beta, v]$ to the scale L_1 scarcely differs from the hodograph of vector $\mathbf{K}[\beta, \mu]$, shown in Figs. 1 and 2.

An analysis of the properties of the system shows that the most favorable conditions for exciting instability exist when the natural frequencies of the lowest harmonics of the structure and of the propellant line are close together. At frequencies close to the natural frequency of the structure ω_n, as follows from (2.4), $\eta_n \gg \eta_c$, $\eta_n \gg \eta_m$ $(n \neq m)$, and we may therefore put, in the first approximation, $\eta_c = \eta_m = 0$ $(m = 1, 2, \ldots, m \neq n)$. In this case the block diagram of the system is simplest; for one propellant line it is as shown in Fig. 9.

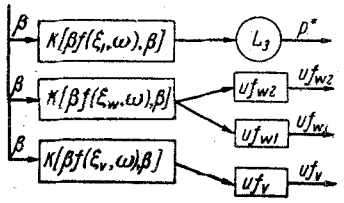

Fig. 7

The complex ratios $\mathbf{K}^*[v, p]$, $\mathbf{K}^*[v, p^*]$ of the equivalent elements for the propellant line may be determined from Fig. 5. The complex ratio $\mathbf{K}^*[v, u]$ presents more difficulty. It may be obtained either from Fig. 5, by combining the effects of uf_{w2}, uf_{w1}, uf_v using (3.4), (3.5), (4.3), or by using the formulas of [9], putting, on the basis of (3.4) and (3.5),

$$f_{w2} = f_{nw}(1 + \lambda_{21}) - \lambda_{21} f_{n1}, \qquad f_{w1} = f_{nw}(1 + \lambda_{12}) - \lambda_{12} f_{nv}$$
$$f_v = f_{nv}(1 + \lambda_{22}) - \lambda_{22} f_{nw}.$$

We obtain a further simplification by replacing elements with complex ratios $\mathbf{K}^*[\beta, v]$, $\mathbf{K}[v, p]$ by the equivalent element (Fig. 10), in which case

$$\mathbf{K}^{**}[\beta, v] = \frac{\mathbf{K}^*[\beta, v]}{1 - \mathbf{K}^*[\beta, v]\,\mathbf{K}^*[v, p] L_2}. \qquad (4.7)$$

The complex ratio $\mathbf{K}^{**}[\beta, v]$ expresses the relation between the variation β of chamber pressure and the variation v of the propellant injection rate, allowing for the reaction of the propellant line on this pressure. Now the variation v

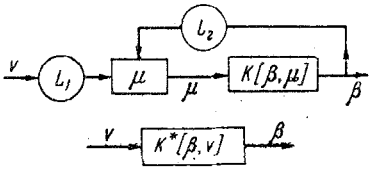

Fig. 8

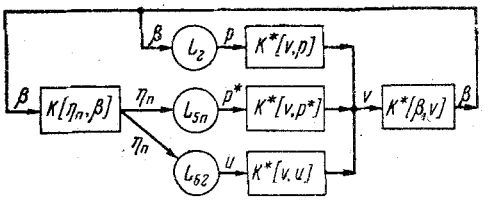

Fig. 9

is due only to the variation of pressure p* upon admission of propellant into the line and to the motion of the pump and the injector head relative to the undisturbed flow, denoted symbolically by the variation of velocity u.

5. Figures 4-10 allow various problems to be solved: effect of the parameters and their combinations on the stability of the system under design conditions, designation of parametric relations calculated to ensure stability, choice and specification of stabilization techniques (including the use of automatic control of propellant supply to the chamber) [11, 12], determination of the permissible region of variation of certain parameters for given values of the remaining parameters, and, finally, allowance for propellant injection oscillations in studies of high-frequency vibrations in the chamber.

The properties of the system depend on a considerable number of physical parameters, many of which are intimately interrelated. For example, due to expenditure of propellant during flight, h_1 and m decrease, Ω_n increases, and the values of f_{n1}, f_{nw}, f_{nv} change. Increase or decrease in the thickness of the tank bottom or changes in the rigidity of the motor suspension lead to variation of the values of Ω_n, f_{n1}, f_{nw}, f_{nv}. In the general case, therefore, analysis of the system becomes very complicated. In practical cases it is simplified somewhat, since one must deal with a specific vehicle and a LRM whose parameters are either known or may be varied within certain limits.

We shall note certain general properties of the system, leaving out peculiarities connected with variation of the many parameters over wide limits. Analysis of the equation

$$1 - \mathbf{K}^*[\beta, v]\,\mathbf{K}^*[v, p] L_2 = 0,$$

which is characteristic of element (4.7), shows that for certain relations between the parameters of the chamber and the propellant line its complex roots lie in the right half-plane and therefore the element (4.7) may be unstable. This agrees with the conclusions of [5].

It is characteristic of the dynamic system that it may be unstable, even if the combustion chamber is considered as an ideal element with $\theta = \tau^\circ = \nu = A = 0$. Formula (4.7) will then be simpler:

$$\mathbf{K}^{**}[\beta, \nu] = \frac{k_0}{1 - \mathbf{K}^{*}[v, p] k_0 L_2}. \tag{5.1}$$

We will establish an important property of the complex ratio $\mathbf{K}^{**}[\beta, \nu]$, which, for clarity, we shall formulate for the case when $\mathbf{K}^{*}[v, p] = \mathbf{K}[v, p]$. We shall consider that at both ends of the tube there are resistances satisfying the conditions $\psi_1 M_1 < 1, \psi_2 M_1 < 1$ (these conditions are always fulfilled in practice). The dimensionless natural oscillation frequency of the liquid flow in the tube is the same as for a tube "open" at both ends [13]; it is equal to $(1 - M_1^2)$ in $(n = 1, 2, \ldots)$.

Since the hodograph of vector K[v, p] lies in the left half-plane of $Z = U + iV$ and the modulus of the vector K[v, p] has a minimum at $s_{1n} = (1 - M_1^2)(2n - 1)\pi / 2$ $(n = 1, 2, \ldots)$, we find from (5.4) that the hodograph of vector $\mathbf{K}^{**}[\beta, \nu]$ will lie in the right half-plane of Z (Fig. 11a); the modulus of this vector attains a maximum at $s_1 = s_{1n}$. This value corresponds to the frequency of the flow in a tube closed at one end. Thus, the presence of feedback at the chamber in the form of a tube "open" at both ends forms an equivalent element whose natural frequency is equal to the frequency of the tube closed at one end. The first natural frequency of the equivalent element (5.1) is lower by a factor of two than the first natural frequency of the liquid flow in the tube between the tank and the chamber.

The stability of the closed system shown in Fig. 10 may conveniently be analyzed using the phase-amplitude criterion [7]. Figure 11 shows a typical form of the phase-amplitude frequency characteristics of elements of a system relating to the simplest case when the propellant line consists of a uniform tube $\mathbf{K}^{*}[v, p^*] = \mathbf{K}[v, p^*]$, $\mathbf{K}^{*}[v, u] = \mathbf{K}[v, u]$ and the combustion chamber is an ieeal element. The curves b, c, d, e represent, respectively, hodographs of the vectors

$$\mathbf{K}[\eta_n, \beta] L_{5n} = A_{p^*} e^{i\varphi_{p^*}},$$
$$\mathbf{K}[\eta_n, \beta] L_{62} = A_u e^{i\varphi_u},$$
$$\mathbf{K}[v, p^*] = A_{vp^*} e^{i\varphi_{vp^*}},$$
$$\mathbf{K}[v, u] = A_{vu} e^{i\varphi_{vu}},$$
$$\mathbf{K}^{**}[\beta, \nu] = A_\beta e^{i\beta}.$$

Each element in Fig. 10, taken separately, is stable, and so the closed system will be unstable only if, for $0 \leqslant s_1 \leqslant \infty$, the open-circuit phase-amplitude characteristic

$$[A_{p^*} A_{vp^*} \exp i(\varphi_{p^*} + \varphi_{vp^*}) + A_u A_{vu} \exp i(\varphi_u + \varphi_{vu})] A_\beta \exp i\beta \tag{5.2}$$

on the plane $Z = U + iV$ includes the point (1, i0).

On the basis of formulas (2.5), (2.6), (3.1), and (3.2) of [9] we may conclude that the moduli of the complex ratios $A_{p^*} A_{vp^*}$, $A_u A_{vu}$ are proportional, respectively, to $n_x f_{n1} f_{nv} h_1 / l$, $n_x f_{nv}^2$, where n_x is the axial load factor of the vehicle. If $f_{nv} = 0$, the circuit breaks down, and a closed system does not exist.

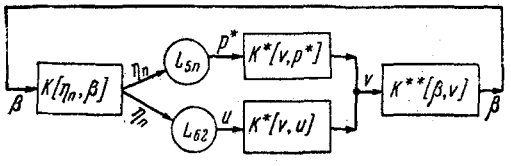

Fig. 10

When $f_{n1} = 0$ $(p^* = 0)$, the system remains closed, and the variation of propellant injection into the chamber is caused by motion of the injector head. As is evident from Fig. 11a, c, e, in the range $0 \leqslant s_1 \leqslant \infty$ there is a value $s_1 = s_1^\circ$, such that $\varphi_u + \varphi_{vu} + \varphi_\beta = 0$. The system will be unstable if $A_u A_{vu} A_\beta > 1$ when $s_1 = s_1^\circ$. The best conditions in a situation of this kind correspond to $\omega_n \approx s_{1n}$.

Mostly, $f_{n1} \neq 0$, $f_{nv} \neq 0$, and variation of propellant injection into the chamber is caused by motion of the bottom of the tank and the injector head. There are two possibilities: $f_{n1} f_{nv} > 0$, the solid curve, and $f_{n1} f_{uv} < 0$, the broken curve in Fig. 11b. It can be established from an analysis of (5.2) and from the curves of Fig. 11 that, in the case $f_{n1} f_{nw} > 0$, the possibility of loss of stability at the lower natural frequencies increases, while for $f_{n1} f_{nw} < 0$ it decreases compared with the case $f_{n1} = 0$. Other conditions being equal, the possibility of exciting instability increases as n_x increases, while for $f_{n1} f_{nv} > 0$, it is greater for greater h_1/l. Damping of the structure (ε_n) and the resistances in the feed line $(\psi_1 M_1, \psi_2 M_1)$ promote stability of motion. The greater the pressure drop in the injectors, the more stable the system.

The stability criteria of the system are less obvious when the chamber cannot be treated as an ideal element and the propellant supply system has a pump. For bipropellant systems they are even harder to discern. For many types of LRM vehicles (particularly with a liquid-reactant gas generator operating on the basic propellants) the dynamic system

is more complicated and may include automatic equipment for controlling the propellant supply to the chamber [4].

The linearized equations will only yield conclusions regarding the stability or instability of the system. If the system is unstable and random oscillations build up, the assumption of linearity becomes invalid. Nonlinearity of the equations for the combustion chamber, the possibility of cavitation effects in the feed lines, etc., lead to a change in the dynamic properties of the system, and a self-oscillating regime may develop in the system.

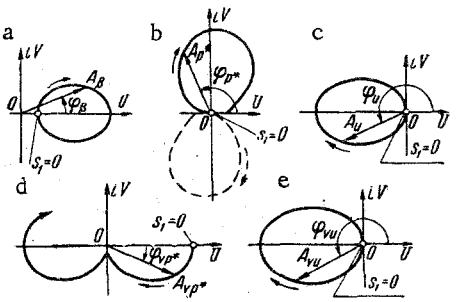

Fig. 11

REFERENCES

1. D. F. Gunder and D. R. Friant, "Stability of flow in a rocket motor.," J. Appl. Mech., vol. 17, 1950.

2. M. Summerfield, "A theory of unstable combustion in liquid propellant rocket systems," J. Amer. Rocket Soc., no. 5, vol. 21, 1951.

3. L. Crocco, "Aspects of combustion stability in liquid propellant rocket motors. Part 1: Fundamentals of low-frequency instability with monopropellants.," J. Amer. Rocket Soc., vol. 21, no. 6, 1951.

4. L. Crocco and Chen Hsin-i, Theory of Combustion Instability in Liquid-Propellant Rocket Motors [Russian translation], IL, 1958.

5. R. H. Sabersky, "Effect of wave propagation in feed lines on low-frequency rocket instability," Jet Propulsion, vol. 24, 1954.

6. R. S. Wick, "The effect of vehicle structure on propulsion system dynamics and stability," Jet Propulsion, vol. 26, no. 10, 1956.

7. E. P. Popov, Dynamics of Automatic Control Systems [in Russian], Gostekhizdat, 1954.

8. V. I. Feodosev and G. B. Sinyarev, Introduction to Missile Engineering [in Russian], Oborongiz, 1960.

9. K. S. Kolesnikov, "Forced oscillations of a perfect compressible liquid injected into a chamber," Izv. AN SSSR, Mekhanika i mashinostroenie, no. 5, 1963.

10. V. Ya. Karelin, Cavitation Phenomena in Centrifugal and Axial Pumps [in Russian], Mashgiz, 1963.

11. Y. T. Li, "Stabilization of low-frequency oscillations of liquid propellant rockets with fuel line stabilizer," Jet Propulsion, vol. 26, no. 1, 1956.

12. Y. C. Dee, A. M. Picles, and C. C. Miesse, "Experimental aspects of rocket system stability," Jet. Propulsion, vol. 26, no. 1, 1956.

13. K. S. Kolesnikov, "Forced oscillations of a perfect compressible liquid flow in a straight uniform tube," Izv. AN SSSR, OTN, Mekhanika i mashinostroenie, no. 4, 1963.

7 December 1963

Moscow